



## New experimental setup for thermoacoustic instabilities investigation in two-phase flow swirled combustion

Marcos Caceres, Françoise Baillot, Eric Domingues, Jean-Bernard Blaisot,  
Gilles Godard, Carole Gobin

### ► To cite this version:

Marcos Caceres, Françoise Baillot, Eric Domingues, Jean-Bernard Blaisot, Gilles Godard, et al.. New experimental setup for thermoacoustic instabilities investigation in two-phase flow swirled combustion. European Combustion Meeting (ECM), Apr 2017, Duvrobnick, Croatia. 6 p. hal-02177230

HAL Id: hal-02177230

<https://normandie-univ.hal.science/hal-02177230>

Submitted on 7 Nov 2019

**HAL** is a multi-disciplinary open access archive for the deposit and dissemination of scientific research documents, whether they are published or not. The documents may come from teaching and research institutions in France or abroad, or from public or private research centers.

L'archive ouverte pluridisciplinaire **HAL**, est destinée au dépôt et à la diffusion de documents scientifiques de niveau recherche, publiés ou non, émanant des établissements d'enseignement et de recherche français ou étrangers, des laboratoires publics ou privés.

# New experimental setup for thermoacoustic instabilities investigation in two-phase flow swirled combustion

M. Cáceres\*, F. Baillot, E. Domingues, J-B. Blaisot, G. Godard, C. Gobin  
Normandie Univ, UNIROUEN, INSA Rouen, CNRS, CORIA, 76000 Rouen, France.

## Abstract

An original experimental setup is designed to study thermoacoustic instabilities in two-phase swirled-flow combustion (air/n-heptane). It is composed of an atmospheric linear multi-injection cavity whose length is adjustable in order to excite resonant chamber acoustic modes by means of an acoustic forcing. Without combustion, a procedure based on experimental, numerical and theoretical results, proposes criteria which show evidence of the presence of the 2T1L mode. Thanks to these criteria the 2T1L mode is revealed with combustion despite of the non-uniform temperature field and non-constant sound speed. The system is validated by quantifying the flame CH\* emission submitted to the 2T1L mode.

## Introduction

Governments and industry players agree that more energy-efficient combustion systems are necessary to help protect our planet: by optimizing energy systems and reducing pollutant emissions. Particularly in aviation transportation, the High Level Group (HLG) on Aviation and Aeronautics Research of the European Commission and the Advisory Council for Aeronautics Research in Europe have set challenging goals, namely 75% fewer CO<sub>2</sub> emissions, 90% fewer NOx emissions and 65% less flying aircraft noise by 2050 compared to 2000 levels [1]. To meet these targets, the technology based on lean burn combustors (e.g. lean-premixed or lean-premixed prevaporized combustors) is one of the most favourable to reach the target of the NOx mitigation while limiting the formation of CO. These energetic systems, featuring increased efficiencies, are promising devices to meet the future requirements [2]. However this technology does not escape to combustion instabilities which hinder its development. Since more air is affected to the injection system, probability to activate hydrodynamic instabilities is increased; as they may enter into the process of combustion instabilities, an interaction with acoustic waves is also increased [3]. In order to eliminate them at the design stage, fundamental mechanisms leading to these instabilities have to be well understood. Moreover, even now, current industrial combustion systems like rocket engines, aeronautical turbines or land-based turbines are subject to combustion unsteadiness, likely to interact with acoustics. In all the cases, the resulting thermoacoustic instabilities are produced generally by longitudinal and/or transverse modes coupled with the heat release rate [4, 5]. Numerical methods to predict and control these instabilities have become very attractive, but they always need experiments to set and validate models. Very few experimental studies are dedicated to multiple liquid fuelled injectors assisted by coaxial swirling air flow submitted to longitudinal acoustic perturbations, and even less, to azimuthal ones. In that framework, it has been designed a new original experimental setup in which longitudinal and/or transverse acoustic waves can be generated and perturb three air/n-heptane flames issued from swirling

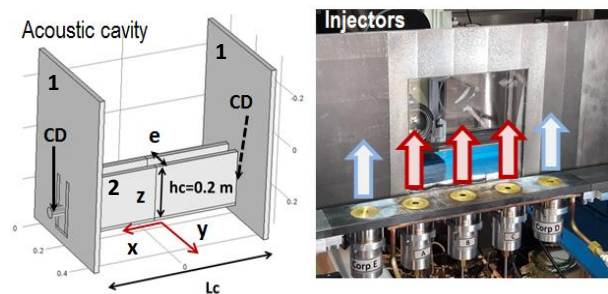


**Fig. 1:** Acoustic cavity (left), compression drivers (CD), 1 – side walls, 2 – front walls. Injector system (right); arrows: red (fuel/air), blue (air).

two-phase flows. Forcing flames and investigating their mutual response contributes to the improvement of understanding of thermoacoustic instabilities occurring in liquid fuelled powered combustors.

## Specific Objectives

The setup was designed in order to ensure combustion inside an atmospheric linear chamber. Acoustic actuators are implemented on two opposite vertical side walls. The first aim was to find a way to protect the actuators from heat release without losing any acoustic efficiency and to ensure the generation of adequate aerodynamic system to stabilize three swirling flames in spite of the presence of a large hole in side walls for letting acoustic waves through. Secondly, the chamber was built to be used as an acoustic cavity tuned to its second resonant transverse mode (2T1L). Main characteristics of the mode obtained without combustion, served to verify the 2T1L mode was well excited with combustion, despite the non-uniform temperature field and non-constant sound speed. Finally, the setup and experimental methodology are validated by showing the flames' response is well coupled to the pressure fluctuations produced by the transverse waves.

## Experimental Setup

**Acoustic cavity:** The chamber is an atmospheric linear multi-injection steel cavity. It represents an unwrapped sector of the annular combustion chamber developed at EM2C laboratory [6]. Fig. 1 shows the

\* Corresponding author: [marcos.caceres@coria.fr](mailto:marcos.caceres@coria.fr)

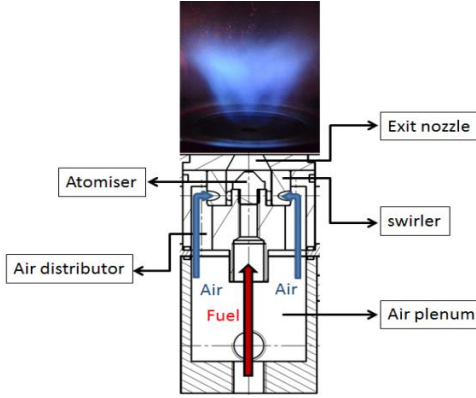


**Fig. 2:** Injector with a two-phase flow swirling flame.

setup composed of a fixed bottom and of four (two side and two front) lateral walls which can be moved by a sliding mechanism. Two face to face quartz windows assembled on front walls allow optical access to the injection zone. The cavity dimensions are defined by: width  $e = 55$  mm, height  $h_c = 200$  mm and adjustable length  $L_c$ . Two compression drivers BEYMA CP850ND, set face to face on the side walls distant by  $L_c$  are used to create acoustic waves inside the cavity.  $L_c$  is chosen in order to force resonant chamber acoustic modes for a given frequency. The acoustic modes in the cavity are also characterized numerically by finite element analysis achieved with software COMSOL Multiphysics<sup>©</sup>.

A point inside the cavity is specified by a Cartesian coordinate system  $(O_c, \mathbf{x}, \mathbf{y}, \mathbf{z})$  where  $O_c$  is the center of the horizontal bottom plate; axis  $(O_c, \mathbf{x})$  is horizontal and  $(O_c, \mathbf{z})$  is the vertical ascending axis. In the following, coordinates  $(x, y, z)$  are non-dimensionalized by  $L_c$ ,  $e$  and  $h_c$  respectively. To prevent any awkwardness in writing, the non-dimensionalized coordinates are still expressed as  $(x, y, z)$ .

*Injection system:* it is mounted on the fixed bottom of the cavity (see red arrows in fig. 1). By using the sliding mechanism the injection system can be placed at various specific locations of the controlled acoustic field. It consists of three independent linearly-arranged radial swirl injectors separated by a center distance  $a_{inj} = 6.5$  mm. As shown in fig. 2, each one is composed of an atomizer for n-heptane and a plenum, a distributor and a swirler for the air. The exit nozzle has a diameter  $D_{exit} = 8$  mm. The three liquid-lines are pressurized by a unique pump Tuthill DGS. The liquid flow rate for each line is controlled by a Coriolis mass flow meter BRONKHORST; the air flow rate for each line is given by a mass flow meter HASTING HFM-201. Operating conditions range in 340 - 450 g/h for  $\dot{m}_f$ , the fuel flow rate, and in 70 - 105 L/min for  $\dot{m}_{air}$ , the air flow rate. These conditions give a global power of about 4.22 kW to 5.59 kW.

*Stabilization system:* In the aforementioned annular chamber (EM2C), the overall stabilization is ensured by a set of swirled flames distributed all around a circumference. Herein, such an intrinsic energetic/aerodynamic equilibrium is not assured because the three injectors are too far from the vertical side walls for them to partici-

pate in their stabilization; thus a method was found to guarantee the combustion persistence. It consists in adding two swirling air jets placed next to the two outer injectors at the same center distance  $a_{inj}$  (see blue arrows in fig. 1). This configuration creates appropriate boundary conditions to stabilize the spray flames. Moreover the two inert jets keep the flames away from side walls where compression drivers are mounted, avoiding their overheating. The driver performances are then unchanged compared to the use at ambient temperature. An example of operating points (used as a test case in section “Research of the 2TIL mode” with combustion) which provides the stabilization of three swirling flames is:  $\dot{m}_{air} = 80$  L/min and  $\dot{m}_f = 400$  g/h for each injector supporting flame;  $\dot{m}_{air} = 175$  L/min and  $\dot{m}_f = 0$  g/h for the two injectors without fuel.

*Cavity instrumentation:* Sets constituted of a thermocouple type K and a microphone B&K type 4182 are installed at various points of the cavity. The microphone is equipped with a stiff tube of diameter  $d_{tube} = 1.2$  mm and length  $L_{tube}$  to keep the sensor away from the hot environment [7]. But this configuration introduces a phase shift  $\varphi_{probe}$  associated to the propagation of the acoustic wave inside the probe tube. The distance between the tube end and the sensor membrane is  $L_{tube} + L_m$  with  $L_m = 13$  mm the connecting element length.  $L_{tube} = 100$  mm is chosen in all the experiments, whatever the temperature environment. In addition a phase-shift of  $\pi$  is added due to the intrinsic electronic inversion. By using the complex formulation, noted  $\langle \cdot \rangle$ , to process signals, pressure fluctuations  $\hat{p}'(\mathbf{x}, t)$  associated to  $p'(\mathbf{x}, t)$  are then deduced from probe measurements  $\hat{p}'_{probe}(\mathbf{x}, t)$  by writing:

$$p'(\mathbf{x}, t) = \hat{p}'_{probe}(\mathbf{x}, t) e^{-i\varphi_{probe}}$$

For a harmonic wave of angular frequency  $\omega$ ,  $\varphi_{probe} = \omega(L_{tube} + L_m)/c(T) + \pi$ .

With combustion, sets of thermocouple and microphone are positioned on the wall at  $y = 0.5$  at several x-locations. Temperature is shown to vary along the cavity (see table 1). The non-uniformity of the temperature field leads to a non-constant sound speed  $c(T)$  inside the chamber. This variation is taken into account to determine the local pressure fluctuations from the pressure measurements  $\hat{p}'_{probe}(\mathbf{x}, t)$  through the correction of the phase  $\varphi_{probe}$ .

**Table 1:** Temperatures measured at  $y = 0.5$ ,  $z = 0.025$  for  $L_c = 800$  mm.

Position	Block n°	Temperature (K)
$x = 0$	5	863
$x = 0.256$	1	358
$x = 0.5$	2	318

## Two-phase flow characterization

*The spray:* n-heptane spray from a single injector was characterized in the presence of a swirling air flow, but without combustion. Droplet sizing at the injector

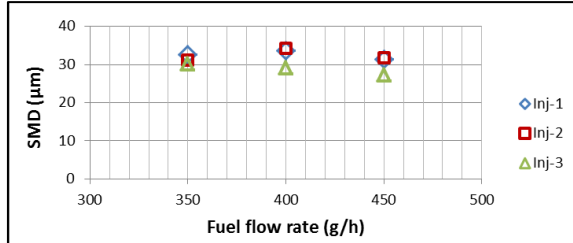


**Fig. 3:** SMD evolution results by laser diffraction for each injector for  $\dot{m}_{air} = 80 \text{ L/min}$ .

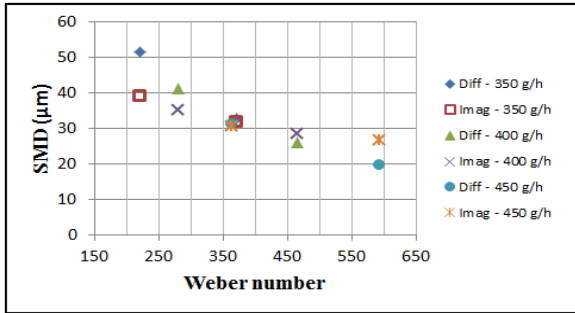


**Fig. 4:** SMD vs. Weber number for a given  $\dot{m}_f$  obtained by laser diffraction imaging.

exit was carried out by laser diffraction (Malvern system). In addition spray was investigated by means of imaging with backlight diffuse-illumination. Comparison of results of both methods shows that the Sauter Mean Diameter (SMD)  $d_{32}$  is independent of the liquid flow rate  $\dot{m}_f$  for a given  $\dot{m}_{air}$  (Fig. 3), and depends inversely on  $\dot{m}_{air}$ . SMD varies here from 50 to 20  $\mu\text{m}$  for  $\dot{m}_{air}$  ranging from 60 to 105 L/min. A better injector atomization is found for high  $\dot{m}_{air}$ . Data are reported in fig. 4 as a function of the Weber number  $We = \rho_{air} U_b^2 D_{inj} / \sigma$ , where  $U_b$  is the bulk air velocity at the injector exit and  $\sigma$  is the surface tension of the n-heptane. Based on the chart of Lasheras and Hopfinger [8], the jet breakup process is placed at the limit of a membrane breakup ( $We < 300$ ) and fiber type atomization ( $We > 300$ ). The Reynolds number used in the chart is defined by  $Re = \rho_{air} U_b D_{inj} / \mu_{air}$  which belongs to the range  $[1 \times 10^4 - 2 \times 10^4]$ .

*The air flow:* Velocity profiles of the air flow were obtained by means of a Phase Doppler Anemometry system (PDA). The case presented here ( $U_b = 23.2 \text{ m/s}$  for  $\dot{m}_{air} = 70 \text{ L/min}$ ) is given as a representative example. The air was seeded upstream by DEHS droplets of diameter  $d_p < 5 \mu\text{m}$  and density  $\rho_p = 0.912 \times 10^3 \text{ kg/m}^3$ . The Stokes number  $S_t$ , is introduced to evaluate how the seeding is able to follow the air flow dynamics. It is defined by  $S_t = \tau_{DEHS} / \tau_{air}$  with  $\tau_{DEHS} = \rho_p d_p^2 / 18 \mu_{air}$  and  $\tau_{air} = D_{ext} / U_b$ . As  $S_t$  is lower than 0.2, the use of this tracer is satisfactory to investigate air flow properties. Fig. 5 shows the mean air velocity profiles  $\{U_z, U_r, U_\theta\}$  measured at  $z = 0.015$ . The data rate of 40 000 droplets/s ensures the convergence of the data. The mean vertical velocity profile presents a central recirculation zone (CRZ). The azimuthal component is of the same order of magnitude as

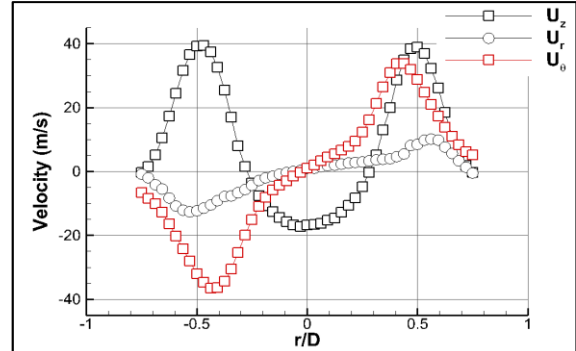


**Fig. 5:** Mean air velocity profiles of the seeded swirling air jet:  $U_z$  (axial),  $U_r$  (radial),  $U_\theta$  (azimuthal).

the vertical component indicating a strong swirl. The swirl number  $S$  is evaluated from eq. 1 [9]. Here  $S$  equals 0.83, which is consistent with the CRZ detection.

$$S = \int_0^R U_z U_\theta r^2 dr / R \int_0^R U_z^2 r dr \quad (1)$$

### Research of the 2T1L mode

The complex formulation of the pressure for a harmonic wave is expressed as  $\hat{p}'(\mathbf{x}, t) = P'(\mathbf{x})e^{i\omega t}$  with  $P'(\mathbf{x}) \in \mathbb{C}$ ; the normalized pressure amplitude is introduced as follows:

$$|P'_{x,y,z}| / |P'_{x,y,z}|_{max} \quad (2)$$

The forcing frequency  $f_0$  ranges between 0.5 and 1.4 kHz. The aim is to excite a transverse acoustic resonant mode of the cavity with combustion having a pressure antinode (PA) at  $x = 0$  (center of the cavity). For that purpose, an experimental procedure is proposed to set the 2T1L mode. It is first validated without combustion.

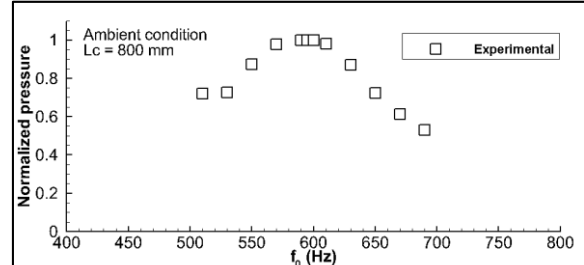


**Fig. 6:** Normalized pressure  $|P'_{0,0,z}| / |P'_{0,0,z}|_{max}$  in the frequency domain. Here  $z = 0.025$ .

*Procedure validating the excitation of the 2T1L mode without combustion:* The procedure is presented by means of some representative examples. To find the resonant modes of the cavity, the frequency forcing is varied successively from 0.5 to 1.4 kHz whilst measuring acoustic pressure amplitude  $|P'_{0,0,z}|$  at the same time. Fig. 6 shows an example for which the normalized pressure amplitude  $|P'_{0,0,z}| / |P'_{0,0,z}|_{max}$  with  $z = 0.025$ , is measured at ambient temperature for  $L_c = 0.8 \text{ m}$ ; the subscript "max" refers to the maximum value obtained in the frequency range of investigation. Open symbols represent experimental data. According to standard acoustic power laws of actuators, the highest peak measured in the present frequency range can be

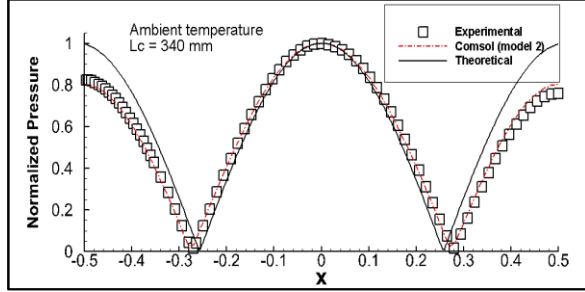


**Fig. 7:** Pressure field measured along  $x$ -axis ( $y = 0, z = 0.025$ ) showing a second order stationary acoustic field,  $f_0 = 1020$  Hz

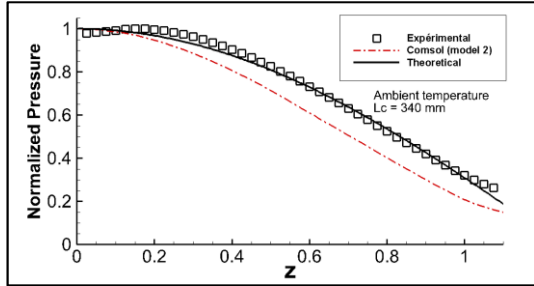


**Fig. 8:** Pressure field measured along  $z$ -axis ( $x = 0, y = 0$ ) showing a quarter wavelength resonance,  $f_0 = 1020$  Hz

recognized as the 2T1L resonant mode of the cavity. This is corroborated by the experimental and numerical cross-validation, illustrated in figs. 7 and 8 for the case  $L_c = 0.34$  m. In addition to calculations, fig. 7 reports experimental data obtained along  $x$ -axis ( $y = 0, z = 0.025$ ) and fig. 8 reports data along  $z$ -axis ( $x = 0, y = 0$ ). Simulations match well with experimental data which show a spatial acoustic response similar to a 2T1L mode. In particular, results indicate that the variation along  $x$  is associated to a standing wave while with  $z$  they are associated to a quarter wavelength resonator behavior (fig. 8). A rough boundary condition imposed at the limit of the domain explains the shift between simulation and experiment in fig. 8. Otherwise  $|P'|$  was also verified to be constant in the  $y$ -direction for any given couples  $(x, z)$ . Finally, the theoretical acoustic pressure amplitude characterizing the mode 2T1L whose frequency is expressed by eq. 3 with wave-number components  $k_x, k_y, k_z$  defined by  $m_x = 2$ ,  $n_y = 0$  and  $p_z = 0$  respectively is compared to experimental and numerical data. The theoretical solution added in figs. 7 and 8 (solid line) agrees satisfactorily with them. The discrepancy next to  $x = \pm 0.5$  in fig. 7 comes from the presence of the compression drivers mounted on the holed side walls, which deviates the response from a pure closed resonator in the  $x$ -direction. But the central zone of interest is well approached by the transverse/longitudinal standing wave.

$$f_{m_x, n_y, p_z} = c_0(T) \left[ \left( \frac{m_x}{2L_c} \right)^2 + \left( \frac{n_y}{2e} \right)^2 + \left( \frac{2p_z+1}{4h_c} \right)^2 \right]^{1/2} \quad (3)$$

Characteristics of such a resonant transverse standing acoustic field were described in previous works [10],

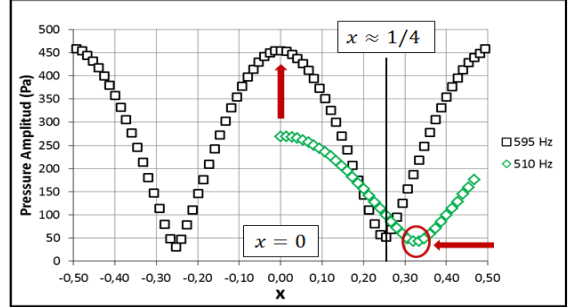


**Fig. 9:** VA moves toward  $x = 1/4$  and  $|P'_{0,0,z}|$  grows towards  $|P'_{0,0,z}|_{\max}$ ,  $L_c = 0.75$  m.

[11] for a semi-open cavity where the environment was unmodified by combustion. For  $f_0 = f_r$  with  $f_r$  the resonant frequency, there is a pressure antinode (PA) at  $x = 0$  where the phase of the pressure fluctuation taken as the reference is null, and two velocity antinodes (VA) associated to pressure minima placed in the experiment at  $x_{VA}$  with  $|1/4| < |x_{VA}| \leq 1.1 |1/4|$ . The phase of the pressure fluctuations  $\varphi(f_r, x)$  around  $x_{VA}$  evolves continuously from 0 to  $\pi$  with  $\varphi(f_r, x_{VA}) = 0.5\pi$  [12]. In the present study it has been noted that when the forcing frequency  $f_0$  is varied by approaching  $f_r$ , the 2T1L mode frequency, the minimum of the pressure amplitude moves its position  $x_{min}$  toward  $x = 1/4$  while the pressure amplitude  $|P'_{0,y,z}|$  in the center of the cavity grows up to  $|P'_{0,y,z}|_{\max}$ . This is indicated by red arrows in fig. 9, reporting a representative experimental example ( $L_c = 0.75$  m). During the pressure minimum's displacement, its phase always satisfies  $\varphi(f_0, x_{min}) = 0.5\pi$ .

To simplify the search and identification of the 2T1L mode, the study has been carried out in the frequency domain.  $|P'_{0,y,z}|$  is measured in the centre of the cavity while phase  $\varphi(f_0, x)$  of the pressure fluctuations is measured at a point of coordinate  $x$  chosen in the vicinity of  $(x = 1/4, y, z)$  located in the basin of the pressure minima as  $f_0$  is varied. The profile of  $|P'_{0,y,z}|$  versus  $f_0$  shows a maximum at  $f_0 = f_r$  while the profile of the phase passes from 0 to  $\pi$ . Identifying a 2T1L acoustic mode is then possible provided that the two following conditions are satisfied as  $f_0$  is varied:

- 1-  $f_0$  is considered as the resonance frequency  $f_r$  when  $|P'_{0,y,z}|$  is maximum ( $|P'_{0,y,z}| = |P'_{0,y,z}|_{\max}$ );
- 2- The phase  $\varphi(f_0, x)$  measured at any fixed point in the vicinity of  $x = 1/4$  (located in the basin of the pressure minima) must vary from 0 to  $\pi$ .

When these conditions are satisfied,  $f_0 = f_r$  for 2T1L mode. The procedure is tested with the example presented afterwards for which  $L_c = 0.8$  m. In fig. 6 it is highlighted that  $|P'_{0,0,z}| = |P'_{0,0,z}|_{\max}$  at 600 Hz. Then, in fig. 10, when  $f_0$  is varied,  $\varphi(f_0, x = 0.256)$  varies from 0 to  $\pi$  and the profile  $|P'_{0.256,0,z}| / |P'_{0,0,z}|$  shows a minimum. So  $f_0 = f_r = 600$  Hz is retained. Once the frequency  $f_r$  is determined, the position  $x_{VA}$  of VA can

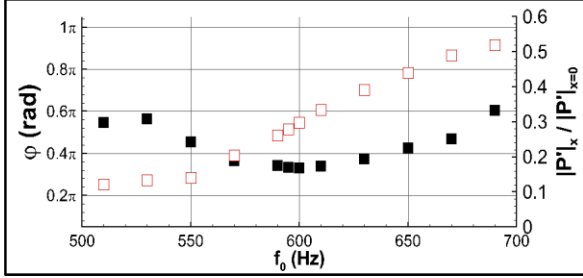


**Fig. 10:**  $|P'_{0.256,0,z}|/|P'_{0,0,z}|$  (■),  $\varphi(f_0, x = 0.256)$  (□).  $L_c = 0.8$  m, w/o flames.

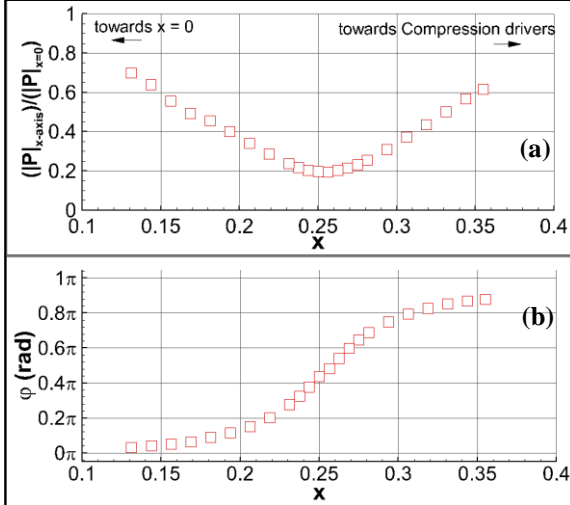


**Fig. 11:** (a)  $|P'_{x,0,0.025}|/|P'_{0,0.5,0.025}|_{\max}$ ; (b)  $\varphi(f_r, x)$ .  $f_r = 600$  Hz,  $L_c = 0.8$  m, w/o flames.

be identified by studying the response of the pressure fluctuations in the spatial domain, namely in the vicinity of  $x = 1/4$ . It is localized where the pressure amplitude is minimum<sup>(1)</sup> with  $\varphi(f_r, x_{VA}) = 0.5\pi$ . From fig. 11 it can be extracted that  $x_{VA} = 0.256$ . Once the procedure validated, it is applied to configurations with combustion.

*With combustion:* The following results are given for a cavity length  $L_c = 0.8$  m and operating conditions given in subsection “*Stabilisation system*”. Pressure is measured by implementing microphones at two points: ( $x = 0, y = 0.5, z = 0.025$ ) and ( $x = 0.256, y = 0.5, z = 0.025$ ). Fig. 12 shows the experimental curve  $|P'_{0,y,z}|/|P'_{0,y,z}|_{\max}$  versus  $f_0$ . The maximum is specified at  $f_0 = 650$  Hz. The excitation of mode 2T1L is validated at this frequency if  $\varphi(f_0, x)$  measured at a fixed point of coordinate  $x$  situated in the vicinity of  $x = 1/4$  (located in the basin of the pressure minima), varies from 0 to  $\pi$ . Ratio  $|P'_{0.256,y,z}|/|P'_{0,y,z}|$  and  $\varphi(f_0, x = 0.256)$  are reported in fig. 13 as functions of  $f_0$ . It is verified that  $\varphi(f_0, x = 0.256)$  varies from 0 to  $\pi$  and the profile  $|P'_{0.256,y,z}|/|P'_{0,y,z}|$  has a minimum<sup>2</sup>.

<sup>1</sup>It can be verified that this minimum is an absolute minimum among the local minima of the pressure amplitudes obtained by varying  $f_0$ .

<sup>2</sup> $x_{min} = 0.256$  is the position of a local minimum associated to the forcing frequency 710Hz, but not the velocity antinode position  $x_{VA}$

Therefore the acoustic mode 2T1L is well excited at  $f_0 = 650$  Hz.

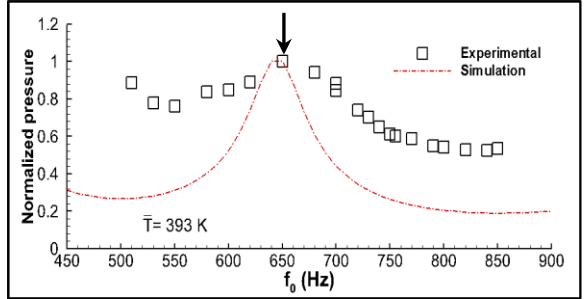


**Fig. 12:**  $|P'_{0,y,z}|/|P'_{0,y,z}|_{\max}$  vs.  $f_0$ . Arrow:  $f_r = 650$  Hz.  $L_c = 0.8$  m, with flames.

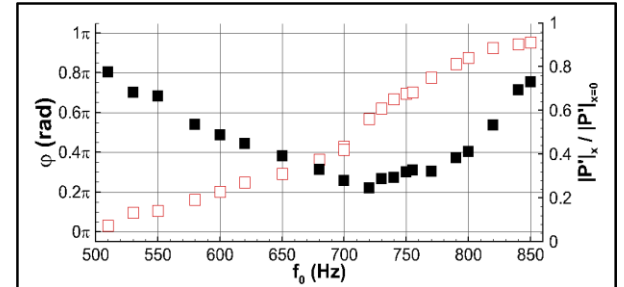


**Fig. 13:**  $|P'_{0.256,0,z}|/|P'_{0,0,z}|$  (■),  $\varphi(f_0, x = 0.256)$  (□).  $L_c = 0.8$  m, with flames.

To complete the method, an equivalent thermal system with a constant temperature  $\bar{T}$  is simulated such that its pressure amplitude response to the forcing frequencies corresponds to the one obtained experimentally. For that purpose, the mean sound speed which depends on  $\bar{T}$ , an unknown temperature is increased until the frequency peak of the simulated profile coincides with the experimental peak. An illustration is given in Fig. 12 on the basis of the previous example; it is found  $\bar{T} = 393$  K<sup>(3)</sup>. Finally this mean temperature field is used to describe the experimental temperature field by a blocks approach based on  $T_j$ , the temperatures measured by thermocouples. The following relationship is introduced:

$$\bar{T} \equiv \frac{\int_0^{L_c} T dx}{L_c} = \sum_{j=1}^{j=n_0} T_j \left( \frac{a_j}{L_c} \right) \quad (4)$$

$n_0$  is the number of blocks by which the cavity is divided; length  $a_j$  of block  $j$  is defined by  $a_j = w_j a$  with  $a = L_c/n_0$  and  $\sum_{j=1}^{j=n_0} w_j = n_0$ . Parameters  $w_j$  weight the influence of  $T_j$ . For the example used above ( $L_c = 0.8$  m and  $T_j$  given in table 1), it is found for  $n_0 = 5$ ,  $w_{j \neq 5} = 1.119$  and  $w_5 = 0.524$ . These weights

the searched 2T1L mode associated to 650Hz. Here the precise localisation  $x_{VA}$  is not looked for.

<sup>3</sup>As 2T1L is tuned while keeping unchanged the cavity geometry,  $k = \sqrt{k_x^2 + k_y^2 + k_z^2}$  is also unchanged provided that the sound speed is constant. By substituting for  $\bar{c}$  obtained from  $\bar{T} = 393$  K in eq. 3, it is deduced  $f_r = 686$  Hz, a value consistent with simulations.

will be used to facilitate the search of an unknown mode 2T1L associated to any distance  $L_c$  and set of measured temperatures  $T_j$  with combustion.

### Application: flame response to a forcing at 650Hz

Three flames are stabilized under the conditions mentioned in section “*Experimental setup*”. The injector system is placed in the centre of the cavity. A photomultiplier (PM) Hamamatsu H6779 records the CH\* radical emission signal from all the flames. The PM is equipped with an interferential filter centered at  $\lambda = 430 \text{ nm}$  with a full width at half maximum  $\Delta\lambda = (10 \pm 2) \text{ nm}$ . In the absence of soot the signal can be directly linked to the heat release rate of the combustion [13].

W/o acoustics the power spectral density of the CH\* signal does not present any particular frequency. With acoustics, the 2T1L mode is excited by imposing  $f_0 = 650\text{Hz}$  for  $L_c = 0.8 \text{ m}$ . The injection system being in the centre of the cavity, the central flame is at the pressure antinode. The CH\* signal recording is synchronized with pressure fluctuation measurements. The CH\* signal modulation is in phase with pressure fluctuations (see fig. 14). In such a case, the Rayleigh criterion is satisfied, which means that instabilities could be driven.

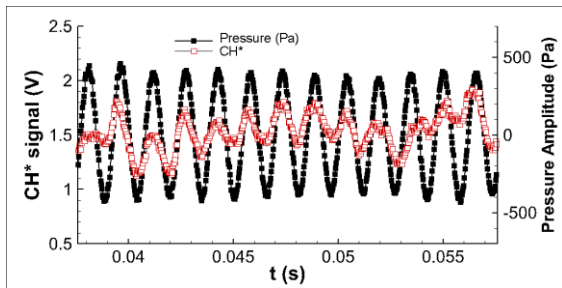


**Fig. 14:**  $P'_{0,y,z}$  and CH\* signals modulated at  $f_0 = 650\text{Hz}$ .

### Conclusion

A new setup has been designed to stabilize three flames produced by swirling two-phase flows linearly arranged in a combustion chamber. An ingenious aerodynamic injection arrangement ensures the persistence of the combustion. The cavity, with an adjustable length  $L_c$ , has been conceived to obtain the resonance of the 2T1L mode for any forcing frequencies  $f_0$  generated in the range [0.5-1.4 kHz] by means of two compression drivers mounted on two opposite walls of the chamber. The experimental response of the cavity with  $f_0$  is well reproduced by simulations and can be interpreted by means of a simplified theoretical calculation. For a given length  $L_c$ , as  $f_0$  is approaching the frequency at the resonance  $f_r$ , the pressure amplitude  $|P'_{0,y,z}|$  in the centre of the cavity grows and the minimum of the pressure amplitudes moves its position  $x_{min}$  toward  $x = 1/4$ . Simultaneously, the phase  $\varphi(f_0, x)$  of the pressure fluctuations measured at a fixed point  $(x, y, z)$  located in the vicinity of  $x = 1/4$ , passes from 0 to  $\pi$

when the forcing frequency varies from  $f_0 < f_r$  to  $f_0 > f_r$ . At  $f_0 = f_r$ ,  $|P'_{0,y,z}|$  defines the pressure antinode amplitude of mode 2T1L and its velocity antinode VA is positioned at  $x_{VA} = x_{min}$  where acoustic pressure fluctuations are an absolute pressure minimum satisfying  $\varphi(f_r, x_{VA}) = 0.5\pi$ .

Based on the abovementioned characteristics, a method has been proposed to determine whether the 2T1L mode is well excited with or without combustion. The defined criterion is based on pressure measurements made at two points in the forcing frequency domain:  $(x = 0, y, z)$  located in the center of the cavity and another one in the vicinity of  $x = 1/4$ . The maximum of pressure amplitude  $|P'_{0,y,z}|$  is searched by varying  $f_0$ . To confirm the identified frequency corresponds to a 2T1L mode,  $\varphi(f_0, x)$  is verified to pass from 0 to  $\pi$  at any point  $x$  near to  $x = 1/4$ . Once the method validated, it is quantified that the flames’ response can be coupled to the pressure fluctuations produced by the transverse waves at the resonant 2T1L mode. In particular CH\* emission is shown to be modulated in phase with them, satisfying the Rayleigh criterion.

### References

- [1] Flightpath 2050 Europe’s Vision for Aviation, Report of the High Level Group on Aviation Research, (2011).
- [2] Y. Huang, V. Yang, Prog. Energy and Combust. Sci. 35 (2009) 293-364.
- [3] M.I. Cazalens, S. Roux, C. Sensiau, T. Poinsot, J. Prop. and Power. 24 (2008) 770-778
- [4] F. Culick, Unsteady Motions in Combustion Chambers for Propulsion Systems, NATO, 2006.
- [5] J. O’Connor, V. Acharya, T. Lieuwen, J. Eng. Gas. Turb. Power (2014).
- [6] D. Durox, K. Prieur, T. Schuller, S. Candel, Procc. ASME Turbo Expo 2015, Paper GT2015-42034, Montreal, Canada, 2015.
- [7] Brüel & Kjær Product data. Probe Microphone type 4182.
- [8] J.C. Lasheras, E.J. Hopfinger, Ann. Rev. Fluid Mech. (2000) 275-308.
- [9] D. Durox, J.P. Moeck, J-F. Bourgouin, P. Moreton, M. Viallon, T. Schuller, S. Candel, Comb. Flame 160 (2013) 1729-1742.
- [10] F. Baillot, F. Lespinasse, Comb. Flame 161 (2014) 1247–1267.
- [11] F. Lespinasse, F. Baillot, T. Boushaki, C. R. Mécanique 341 (2013) 110–120.
- [12] F. Lespinasse, Réponse de la dynamique d’une flamme pré-mélangée à des modes acoustique transverses, Ph.D. thesis, Normandie University, 2014.
- [13] C. Mirat, D. Durox, T. Schuller, Procc. ASME Turbo Expo 2014, Paper GT2014-25111, Düsseldorf, Germany, 2014.